Prediction of the J_C (B) Behavior of Bi-2212 Wires at High Field

Michael D. Brown, Jianyi Jiang, *Senior Member, IEEE*, Chiara Tarantini, Dmytro Abraimov, Griffin Bradford, Jan Jaroszynski, Eric E. Hellstrom, *Senior Member, IEEE*, and David C. Larbalestier, *Fellow, IEEE*

***Abstract*—Bi-2212 wires have been produced for much of the last decade with varying architectures, powder sources, and great variability of final $J_C(B)$ properties. As Bi-2212 transitions from an R&D materials development to a magnet technology, means to predictably forecast $J_C(B)$ becomes increasingly valuable. Here we report on characterizations of short samples having $J_C(15\ \mathrm{T},\ 4.2\ \mathrm{K})$ varying from 1210 to 6560 A/mm^2, measured in fields up to 31 T, and drawn from 10 billets. Using both 4 K transport and variable temperature vibrating sample magnetometer measurements, capable of probing the 20 K irreversibility field, $B_{\mathrm{irr}} = \mu_0 H_k$, we found that the vortex pinning properties are very stable across these wires, which all used the same standard powder composition ($Bi_{2.17}Sr_{1.94}Ca_{0.89}Cu_{2.00}O_{8+x}$), even though it has been made by three different manufacturers over nine years. We conclude that a power-law fit $J_C \propto B^{-\alpha}$, where $\alpha = 0.280$ ($\sigma = 0.015$), works well at 4.2 K over the field range of at least 3–30 T and that $\mu_0 H_k(20\ \mathrm{K})$ remains stable at 8.6 $\pm$ 0.4 T. We conclude that the dominant current limiting mechanism predicting $J_C(B)$ in Bi-2212 is the effective filament connectivity. $J_C(B)$ at high fields may thus be predicted by simple I_C measurements at easily accessible fields in the 3–15 T range.**

***Index Terms*—Bi-2212, critical current density, high-temperature superconductor, multifilamentary wire.**

I. Introduction

EVER since their discovery in the late 1980s, the cuprate "high temperature" superconductors (HTS) have served to light a path towards the generation of high fields above those attainable by their low temperature superconductor (LTS) predecessors. The LTS workhorse conductors Nb-Ti and Nb_3Sn have been used extensively in magnet technology for the last fifty years [1], but they are limited by critical irreversibility fields, $\mu_0 H_{irr}(4.2\,K)$ of ~11 T and ~24 T respectively [2], [3]. If we aim to generate and maintain fields above 24 T, HTS materials are required. After about a decade of conductor development, multiple applications for Bi-2212 appear possible, including solenoid magnets for standard laboratory use and for NMR applications, and accelerator dipoles. The purpose of this paper is to motivate designs of magnets in the 20–40 T range by exploring the predictability of field-dependent critical current density $J_C(B)$.

Presently, HTS conductors can be fabricated as anisotropic tapes (REBCO, Bi-2223) or as an isotropic round wire (Bi-2212), and many important magnet technologies rely on the use of cabled superconductors. Rutherford cable and Cable in Conduit Conductors (CICC) are some of the most common forms for cabling round wire LTS conductors and they have been used extensively in various magnet projects such as the Large Hadron Collider (LHC) [1], [4] and the International Thermonuclear Experimental Reactor (ITER) [5], [6] respectively. To use these well-established LTS cabling technologies for HTS materials, an isotropic round wire is needed, for which Bi-2212 is the only suitable HTS candidate. Great strides have recently been made in the processing of Rutherford-cabled Bi-2212 coils that show superior behavior with respect to training and quench stability when compared to similar LTS coils [7], [8]. Notable is the ability of the optimally processed wire to maintain high whole wire critical current densities, J_E, upwards of $1000\ \mathrm{A/mm^2}$ in a background field of 27 T, highly desirable properties for magnet use.

In the past, ultra-high field data (>15 T) for Bi-2212 round wire has been lacking, as opposed to the more common metrics at 5 T and 15 T. As further improvements to the processing and mechanical support of Bi-2212 coils leads to higher fields, a need arises for dependable $J_C(B)$ metrics up to at least 30 T.

Having made measurements of many wires produced in the last decade, we wished to discover if the variations seen in $J_C(5T)$ and $J_C(15T)$ from wire to wire could be ascribed to connectivity, pinning, or to both. With this in mind, we have measured critical currents for a large data set of Bi-2212 wires up to 31 T, presented here in hopes of illuminating the cause of their variability. We present simple fits to the data that should greatly simplify extrapolation of high field behavior from low field data.

II. Experimental Details

A. Sample Set

To make a comprehensive survey of wire design and precursor types in the last nine years, wires from billets dating from 2009

Manuscript received October 31, 2018; accepted February 1, 2019. Date of publication February 13, 2019; date of current version March 8, 2019. This work was supported by the U.S. Department of Energy, Office of High Energy Physics under Grant DE-SC0010421, from the NHMFL, which was supported by the NSF (NSF/DMR-1644779), and by the State of Florida. *(Corresponding author: Michael D. Brown.)*

The authors are with the Applied Superconductivity Center, National High Magnetic Field Laboratory, Tallahassee, FL 32310 USA, and also with the Florida State University, Tallahassee, FL 32306 USA (e-mail: mdb06h@my.fsu.edu).

Color versions of one or more of the figures in this paper are available online at http://ieeexplore.ieee.org.

Digital Object Identifier 10.1109/TASC.2019.2899226

TABLE I
LIST OF SAMPLES AND VARIOUS RELEVANT SPECIFICATIONS

Wire ID	Architecture [-]	Dia. [mm]	Fill Factor (Densified)	Wire Source [-]	Precursor[a] [-]	Precursor Type [-]	J_C (15T) [A·mm^{-2}]
W1	37 x 18	0.8	0.237	OST/VHFSMC	M1-P1	granulate	1874
W2-1	37 x 18	0.8	0.215	OST/VHFSMC	M1-P1	granulate	1823
W2-2	37 x 18	0.8	0.215	OST/VHFSMC	M1-P1	granulate	2108
W3	37 x 18	0.8	0.253	OST/VHFSMC	M1-P2	powder	1846
W4	37 x 18	0.8	0.236	OST/VHFSMC	M1-P1	granulate	2736
W5	37 x 18	0.8	0.237	OST/VHFSMC	M1-P1	granulate	2217
W6-1	37 x 18	0.8	0.254	OST/VHFSMC	M1-P1	granulate	2677
W6-2	37 x 18	0.8	0.254	OST/VHFSMC	M1-P1	granulate	3171
W7	37 x 18	0.8	0.221	OST/CDP	M1-P3	granulate	1382
W8-1	55 x 18	0.8	0.269	OST/CDP	M2-P4	powder	1210
W8-2	55 x 18	0.8	0.269	OST/CDP	M2-P4	powder	2083
W9-1	55 x 18	0.8	0.198	OST/CDP	M3-P5	powder	3959
W9-2	55 x 18	0.8	0.198	OST/CDP	M3-P5	powder	2581
W9-3	55 x 18	0.8	0.198	OST/CDP	M3-P5	powder	2347
W10-1	55 x 18	0.8	0.199	B-OST/SBIR	M3-P5	powder	5285
W10-2	55 x 18	0.8	0.199	B-OST/SBIR	M3-P5	powder	4101
W10-3	55 x 18	0.8	0.199	B-OST/SBIR	M3-P5	powder	6560

[a]Precursor designation determined by manufacturer (M#), and lot number or precursor type (P#). (i.e., M1-P1 and M1-P2 differ by precursor type. M1-P3 differs from those by lot number. M2-P4 and M3-P5 differ from the others and one another by the source of the precursor.)

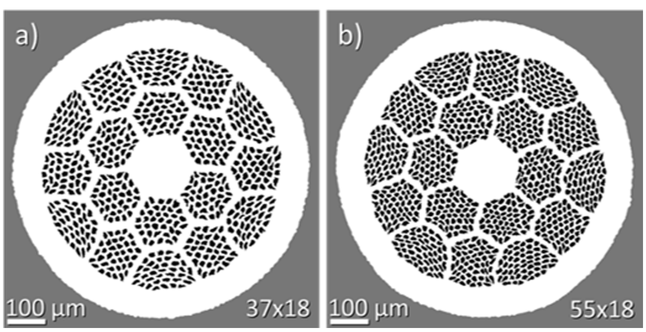

Fig. 1. Architectures of the two principal wire types of this study, (a) 37 × 18 wire (pmm130723-2) with 666 filaments and (b) wire pmm160524 with 990 filaments arrayed in a 55 × 18 array. Both wires were manufactured by Oxford Superconducting Technology, Carteret NJ.

to the present have been included. Table I gives an overview of the wires covered in this study and their specifications. In all, there are five different powder types from three manufactures: Nexans, MetaMateria, and nGimat. All as-drawn wires were produced by Oxford Superconducting Technologies (i.e., OST, now Bruker-OST) using a double-stack Powder-in-Tube (PIT) process. The wires vary between two architectures: 37 × 18 and 55 × 18, containing 666 and 990 filaments respectively. Example cross-sections of densified (but unreacted) wires with these two architectures can be seen in Fig. 1. All the wires have an as-drawn diameter of 0.8 mm.

B. Heat Treatment

Short samples were prepared for testing at the Applied Superconductivity Center (ASC) using a standard overpressure heat treatment (OPHT) schedule [9], [10]. Some samples also received a pre-densification heat treatment immediately before OPHT (PD-OPHT). The OPHT process applies a pressure of 50 bar (1 bar pO_2, balance Ar) throughout the whole heat treatment to prevent dedensification when the Bi-2212 powder is melted at ∼890 °C for a brief period. After melting there is a crucial slow cooling step which allows the recrystallization of the Bi-2212 into a biaxially aligned, large-grain-size morphology that develops the highest critical current density. If a sample is pre-densified, it is subjected to a temperature of 830 °C for 12 hours at 50 bar (5 bar pO_2, balance Ar) for 2 hours before reaction. Sample wires were cut into 15 cm lengths and their ends sealed to allow densification under the OPHT. The end sealing procedure was verified by checking the diameter of the short samples after OPHT, which show a diameter reduction of ∼4% when samples are correctly densified.

C. Critical Current (I_C) Measurements

All high field critical current data were acquired using the four-point probe method in various background fields generated by the 31 T, 50 mm bore magnet at the National High Magnetic Field Laboratory (NHMFL). Samples were cut to a length of 35 mm and mounted horizontally to fit within the 37 mm diameter cryostat. Voltage taps were placed 7 mm apart in the center of the sample and I_C was defined by a voltage criterion of 1 μV/cm.

Above 20 T, a complication often arose because a helium gas bubble can be trapped around the sample by the strong diamagnetism of He gas in high fields in the presence of a strong field gradient when the product $B_Z \cdot dB_Z/dz < -2100\,\mathrm{T}^2/\mathrm{m}$ [11], [12]. Mitigating the problem requires reducing the field below ∼19 T so as to allow the He bubble to rise out of the sample space as normally occurs at lower fields. Consequently, for all measurements above 20 T, the field was first reduced below 19 T and then quickly increased (as is possible with resistive magnets) to the measurement field before taking the I_c data.

D. Magnetization

Magnetization measurements were taken in a vibrating sample magnetometer (VSM) at multiple temperatures between

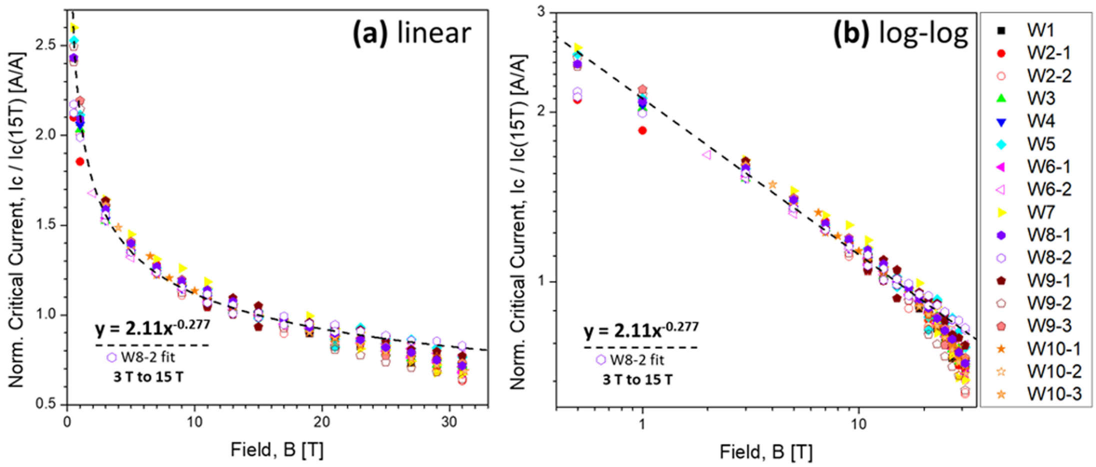

Fig. 2. Plots of $J_C(B)$ data for Bi-2212 wires up to 31 T, normalized to their values at 15 T. Plot (a) is shown in linear scale and plot (b) in log-log scale. Both contain a power law fit from 3 T to 15 T of W8-2 which works well up to 31 T. The value by which each curve is normalized is an averaged value for all measurements taken for the given sample at 15 T.

4.2 K and 20 K in a swept field from -2 T to 14 T. Samples were cut to 5 mm in length and oriented with their axes orthogonal to the field direction.

III. Results

A. Critical Current (I_C) Measurements

Fig. 2 shows data for critical current (I_C) vs applied magnetic field ($B = \mu_0 H$) in both linear and log-log scales with I_C normalized to values at 15 T for all wires from Table I. Note that most curves tend to show power law behavior in the region between ∼3 T and ∼19 T, while some show the behavior to higher fields, with one wire in particular, W8-2, exhibiting power law behavior to 31 T. The power law fit from 3 T to 15 T for the W8-2 wire is shown as a dotted line on both plots in Fig. 2. We note that many data points begin to scatter downward below the power law fit in the He bubble range above ∼20 T, when we assume that significant heating of the wire takes place as the critical current is reached.

B. Power Law Fit

For each wire, values of α were found for the ranges 3 T to 13 T, 15 T, 17 T, etc. up to 31 T to evaluate how α changes as we approach the helium bubble region. Average values of α and their standard deviations for the ranges approaching the helium bubble region (3 T to 15 T, 17 T, and 19 T) were 0.280 ($\sigma = 0.015$), 0.285 ($\sigma = 0.016$), and 0.289 ($\sigma = 0.014$). As seen in Fig. 3, below the helium bubble region, α values for most wires are independent of the upper field limit of the fit. Above ∼20 T the data begin to scatter upward, consistent with sample heating during measurement in the presence of the bubble in the sample space.

C. Magnetization

To complement the 4.2 K transport measurements where, even at 31 T, F_{Pmax} could not be reached, we also ran magnetization up to 14 T at various temperatures from 4.2 to 20 K to check for

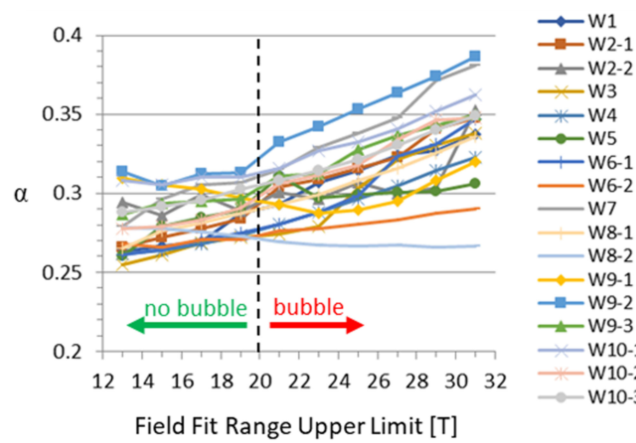

Fig. 3. Plot showing the change in α as the upper limit of the field fit changes between 15 T to 31 T. The average value for α before the He bubble at 19 T is 0.289 ($\sigma = 0.014$).

scaling of the bulk pinning force. The data was normalized at lower temperature by F_{Pmax} or at higher temperatures also by the irreversibility field $\mu_0 H_k$ determined by Kramer function extrapolations. Fig. 4(a) compares the behavior of two of the newer wires, W8-2 and W10-1 made with powders sourced from two different manufacturers (M2-P4 and M3-P5). The data sets from 10–20 K overlap well, suggesting a pinning landscape that is independent of temperature and similar for both powder types and wire types. Fig. 4(b) shows similar data from 4.2 to 20 K. At 4.2 K, neither the field at which F_{Pmax} occurred or $\mu_0 H_k$ could be attained directly, so $\mu_0 H_k(4.2\,K)$ was determined using an exponential fit to the higher temperature $\mu_0 H_k$ values obtained from 10 to 20 K. F_{Pmax} was then estimated using the curve shapes of the 10 through 20 K measurements.

IV. Discussion

The fits for all ranges are determined by the relation:

$$J_C \propto B^{-\alpha}$$

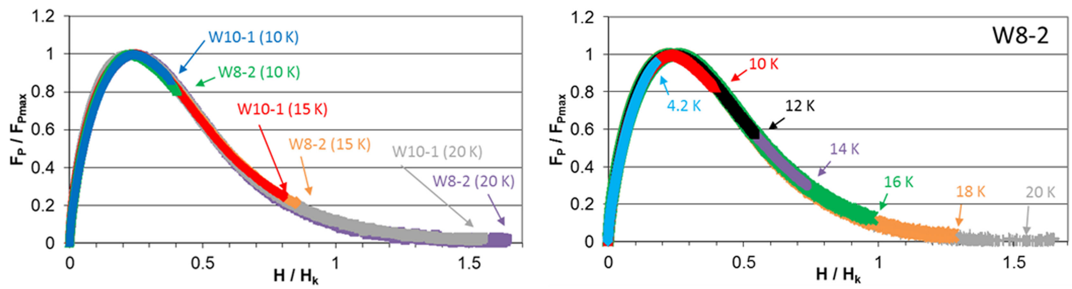

Fig. 4. Normalized bulk pinning force plots ($F_{\mathrm{p}} = J_C$ x B) derived from magnetization measurements (a) comparing two different powder types, W8-1 (with M2-P4) and W10-1 (with M3-P5) and (b) comparing different temperatures from 4.2 K to 20 K for the wire W8-2 (with M2-P4). See Table I for precursor types. The data is normalized by the maximum pinning force for each curve, F_{Pmax}, and the irreversibility field as determined by extrapolations from Kramer plots, H_k.

where B is the field and α is the index which determines the slope of the fit. Such a power law also fits many REBCO coated conductors [13], [14] at 4.2 K at fields up to 31 T for a wide range of orientations at and away from the *c*-axis. Here too we find a broad range over which the pinning parameter α is constant, subject to the experimental complication of lower α when I_c is high and He bubble effects are present. Although α does vary over the range 0.26 to 0.31 before He bubble effects are present, this is a small range compared to our studies of REBCO coated conductors where α ranges from at least 0.7 to almost 1, depending on variations in vortex pinning type and density. We interpret the small range for Bi-2212 as showing that vortex pinning variations are small between different wires, a conclusion reinforced by the small range of $\mu_0 H_k(20\,K)$ values (8.6 $\pm$ 0.4 T) observed for all the samples tested at 20 K by VSM. Given also the great similarity of vortex pinning curve shape seen in Fig. 4, we conclude that there is strong evidence that the dominant variation in $J_C(B)$ is determined by connectivity variations in the Bi-2212 filaments which may be due to small fluctuations in the local density of compressed gas bubbles, heavily misaligned grains or other factors that individually or collectively control the connectivity of the filaments.

Furthermore, 31 T is far below the value for $\mu_0 H_{irr}$ for Bi-2212 suggested by previous studies [15], [16]. This indicates a possibility for measurements from 5 T to 15 T to be used to accurately approximate J_C to ~30 T or even higher fields.

V. Conclusion

We measured a comprehensive set of Bi-2212 wires manufactured over the last decade up to 31 T at 4.2 K by Oxford Superconducting Technology and Bruker-OST using five different powder types produced by three different manufacturers. Values for J_C (15 T) between samples varied by an order of 5 and were as high as 6560 A·mm^{-2}. We found that a power-law fit ($J_C \propto B^{-\alpha}$) is possible between 3 T and 19 T, above which many samples experienced diminished values due to the formation of a trapped He bubble in the sample space which causes sample heating. However, some samples followed the relation up to 31 T. Normalized bulk pinning force plots for different wires showed excellent agreement. We conclude that a power-law fit is a feasible method for estimating $J_C(H)$ at fields up to at least 31 T.

References

[1] L. Bottura, S. A. Gourlay, A. Yamamoto, and A. V. Zlobin, “Superconducting magnets for particle accelerators,” *IEEE Trans. Nucl. Sci.*, vol. 63, no. 2, pp. 751–776, Apr. 2016.
[2] J. A. Parrell, Y. Zhang, M. B. Field, P. Cisek, and S. Hong, “High field $\mathrm{Nb_3Sn}$ conductor development at Oxford superconducting technology,” *IEEE Trans. Appl. Supercond.*, vol. 13, no. 2, pp. 3470–3473, Jun. 2003.
[3] J. A. Parrell, M. B. Field, Y. Zhang, and S. Hong, “Nb_3Sn conductor development for fusion and particle accelerator applications,” *AIP Conf. Proc.*, vol. 711, no. 1, pp. 369–375, Jun. 2004.
[4] F. Savary *et al.*, “The 11 T dipole for HL-LHC: Status and plan,” *IEEE Trans. Appl. Supercond.*, vol. 26, no. 4, Jun. 2016, Art. no. 4005305.
[5] N. Mitchell *et al.*, “The ITER magnet system,” *IEEE Trans. Appl. Supercond.*, vol. 18, no. 2, pp. 435–440, Jun. 2008.
[6] N. Mitchell, A. Devred, P. Libeyre, B. Lim, and F. Savary, “The ITER magnets: Design and construction status,” *IEEE Trans. Appl. Supercond.*, vol. 22, no. 3, Jun. 2012, Art. no. 4200809.
[7] T. Shen *et al.*, “Racetrack coils made of high-temperature superconducting Bi-2212 Rutherford cable operating in a stable and predictable behavior at >8 kA and a wire current density more than 1000 A/mm^2,” Aug. 2018. [Online]. Available: ArXiv180802864.
[8] K. Zhang *et al.*, “Tripled critical current in racetrack coils made of Bi-2212 Rutherford cables with overpressure processing and leakage control,” *Supercond. Sci. Technol.*, vol. 31, no. 10, 2018, Art. no. 105009.
[9] J. Jiang *et al.*, “Effects of filament size on critical current density in overpressure processed Bi-2212 round wire,” *IEEE Trans. Appl. Supercond.*, vol. 27, no. 4, Jun. 2017, Art. no. 6400104.
[10] M. R. Matras, J. Jiang, D. C. Larbalestier, and E. E. Hellstrom, “Understanding the densification process of $Bi_2Sr_2CaCu_2O_X$ round wires with overpressure processing and its effect on critical current density,” *Supercond. Sci. Technol.*, vol. 29, no. 10, 2016, Art. no. 105005.
[11] E. J. McNiff, B. L. Brandt, S. Foner, L. G. Rubin, and R. J. Weggel, “Temperature anomalies observed in liquid 4He columns in magnetic fields with field–field-gradient products >21 T^2/cm,” *Rev. Sci. Instrum.*, vol. 59, no. 11, pp. 2474–2476, Nov. 1988.
[12] H. Bai *et al.*, “Impact of trapped helium gas bubble in liquid helium on the cooling in high magnetic field,” *IEEE Trans. Appl. Supercond.*, vol. 25, no. 3, Jun. 2015, Art. no. 4300104.
[13] A. Xu, V. Braccini, J. Jaroszynski, Y. Xin, and D. C. Larbalestier, “Role of weak uncorrelated pinning introduced by $BaZrO_3$ nanorods at low-temperature in (Y,Gd)$Ba_2Cu_3O_X$ thin films,” *Phys. Rev. B*, vol. 86, no. 11, Sep. 2012, Art. no. 115416.
[14] V. Braccini *et al.*, “Properties of recent IBAD–MOCVD coated conductors relevant to their high field, low temperature magnet use,” *Supercond. Sci. Technol.*, vol. 24, no. 3, Dec. 2010, Art. no. 035001.
[15] J. Jiang, J. Jaroszynski, V. Griffin, N. C. Craig, E. E. Hellstrom, and D. C. Larbalestier, “Irreversibility field of high temperature superconductor Bi-2212,” FSU-NHMFL, ASC, Tallahassee, FL, USA, Res. Rep., 2007.
[16] D. C. Larbalestier *et al.*, “Isotropic round-wire multifilament cuprate superconductor for generation of magnetic fields above 30 T,” *Nature Mater.*, vol. 13, no. 4, pp. 375–381, Apr. 2014.